# Физика

DOI: 10.14529/mmph190108

# FIRST-PRINCIPLES INVESTIGATIONS OF REFERENCE STATES OF $Co_2CrIn$ HEUSLER ALLOYS

***M.A. Zagrebin[1,2,3], V.V. Sokolovskiy[1,3], V.D. Buchelnikov[1,3]***
[1] *Chelyabinsk State University, Chelyabinsk, Russian Federation*
[2] *South Ural State University, Chelyabinsk, Russian Federation*
[3] *National University of Science and Technology "MISiS", Moscow, Russian Federation*
*E-mail: miczag@mail.ru*

**In order to identify the reasons for the differences between the available theoretical and experimental values of the total magnetic moment of $Co_2CrIn$ Heusler alloy, in this work we studied the effects of various magnetic reference states on the magnetic and electronic properties of the alloys by means of *ab initio* and Monte Carlo methods. It is shown that the calculated ground state in the $L2_1$ phase is ferromagnetic. However, the values for both lattice parameter and magnetic moment calculated for the ferrimagnetic state, where the Cr atoms are ordered antiferromagnetically, are found to be in good agreement with the available experimental data. It is shown that the half-metallic behavior is realized only in the case of the ferromagnetic order. By using the calculated exchange coupling parameters in the Heisenberg Hamiltonian, the temperature dependences of magnetization were simulated.**

*Keywords: Heusler alloys; reference states; density of states; exchange parameters.*

## Introduction

Ferromagnetic half-metals (FHM) are potential candidates for applications in spintronic devices because of their high spin polarization of the electron density of states (DOS) at the Fermi level. This means that there is an energy gap in DOS spin configurations. As a result, 100 % of spin-polarized current can be achieved in these materials [1]. Co-based Heusler alloys are promising materials in FHM class, due to their high spin polarization, large energy gaps, high total magnetic moments ($\mu_{tot}$) and Curie temperatures ($T_C$) [2]. Nowadays, the most studied half-metallic Co-based Heusler alloys are $Co_2YZ$ ($Y$ = Cr, Fe, Mn, and $Z$ = Al, Si, Ga, Ge) (for example, see Refs. [2–4] and references therein).

At present, $Co_2CrIn$ alloy is not thoroughly investigated. However, it has attracted huge interest from both experimentalists and theoreticians due to its complex FHM, ferrimagnetic (FIM), and antiferromagnetic (AFM) behaviours. Wurmehl *et al.* [5] reported that $Co_2CrIn$ has the cubic $L2_1$ structure, which can be represented as four interpenetrated *fcc* sublattices. Besides, the magnetization measurements have shown that $Co_2CrIn$ compound has FIM order with the magnetic moment of 1,18 $\mu_B$ at 5 K. In contrast, the calculated value of magnetic moment was found to be 3,16 $\mu_B$ [6]. To find the reasons leading to magnetic moment reduction in $Co_2CrIn$ alloys, we investigated the magnetic ground states in the framework of density functional theory (DFT) and supercell approach. In particular, we studied equilibrium structural, magnetic, and electronic properties of $Co_2CrIn$ compound with different magnetic configurations. To extend obtained magnetic properties from 0 K to finite temperature, we employed classical Monte Carlo (MC) simulations of the Heisenberg model with exchange coupling constants, which were taken from *ab initio* calculations.

This article is organized as follows. Section 2 presents the details of *ab initio* and MC calculations. Section 3 contains the main results. Key results and conclusions are provided at the end of the article (Section 4).

## 1. Calculation details

We performed spin-polarized *ab initio* calculations, using density functional formalism, implemented in the Vienna *ab initio* simulation package (VASP) [7, 8] and the spin-polarized relativistic Korringa–Kohn–Rostoker code (SPR-KKR) [9]. We investigated ground state structural properties, using the pro-

jector augmented wave (PAW) method and supercell approach, realized in VASP. We used the generalized gradient approximation (GGA) in Perdew, Burke and Ernzerhof (PBE) parameterization to describe the exchange-correlation energy [10]. The computational parameters used for modelling in VASP are following. Pseudopotentials were taken for the next electronic configurations: Co($3d^8 4s^1$), Cr($3p^6 3d^5 4s^1$), and In($4d^{10} 5p^1 5s^2$). Kinetic energy cut-off was 400 eV and kinetic energy cut-off for the augmentation charges was 800 eV. The Brillouin zone integration was performed by the Monkhorst-Pack scheme [11] with 8×8×8 k-point sampling for the structure optimization. All performed calculations were semi-relativistic and spin-polarized. Structures were relaxed, using the conjugate gradient algorithm, and both atomic positions and the supercell volume were optimized. To calculate the tetragonal distortions of the cubic structure, we fixed the volume of the supercell as $V_0 = a_0^3 = a^2 c$ .

Cubic $L2_1$ structure was used for ground state calculations. We considered 16-atoms supercell, which consisted of 8 Co, 4 Cr, and 4 In atoms. To find the optimized magnetic order of the austenite structure, we considered three different magnetic states, referred to as FM state (magnetic moments of Co and Cr atoms are parallel), FIM state (two out of four magnetic moments of Cr atoms are reversed), and the AFM state (all magnetic moments of Cr atoms are reversed). We assumed that the magnetic moments of In atoms are negligible. Fig. 1 schematically shows the discussed spin configurations.

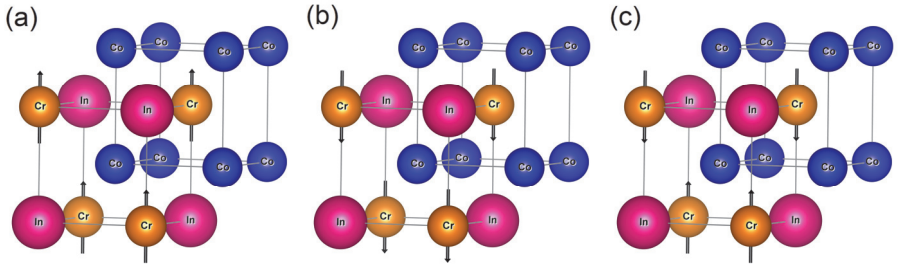


**Fig. 1. $Co_2CrIn$ 16-atom supercells with (a) FM, (b) AFM, (c) FIM spin configurations**

After we defined the equilibrium lattice parameters, we calculated the exchange coupling constants ($J_{ij}$), total and partial DOS, and magnetic moments, using SPR-KKR package. For self-consistent cycles (SCF) calculations, 2300 *k*-points were generated by a *k*-mesh grid of 45×45×45. The angular momentum expansion ($l_{\max}$) was restricted to three. In all calculations total energy converged 0,01 mRy. To achieve the better convergence, we used BROYDEN2 scheme [12, 13] with PBE exchange-correlation potential. We calculated the Heisenberg's projective magnetic exchange coupling constants and DOS curves, using the spin-polarized scalar-relativistic (SP-SREL) Dirac–Hamiltonian with $l_{\max} = 3$ on a *k*-mesh grid of 57×57×57 with 4495 *k* points.

Using obtained long-range exchange coupling constants we simulated the temperature dependencies of magnetization in the framework of classical three-dimensional Heisenberg model and MC routine. For the Hamiltonian we used the following equation:

$$H = -\sum_{i,j} J_{ij} \mathbf{S}_i \mathbf{S}_j \ , \qquad (1)$$

where $\mathbf{S}_i$ is the spin of unit length ($|\mathbf{S}_i| = 1$), placed on a lattice site, and $J_{ij}$ are the exchange coupling parameters from *ab initio* calculations for austenite phase. We carried out MC simulations for a cell with 3925 atoms and periodic boundary conditions, using the Metropolis algorithm [14]. Thus, for a stoichiometric $Co_2CrIn$ alloy, the model lattice contained 1098 Cr, 1099 In, and 1728 Co atoms. Changes of the independent spin variables $\mathbf{S}_i = \{S_i^x, S_i^y, S_i^z\}$ were accepted or rejected according to the single-site transition probability $W = \min\{1;\ \exp(-\Delta H / k_B T)\}$. We used one MC step, consisting of *N* attempts to change the spin variables, as the time unit. For each temperature $5 \cdot 10^5$ MC steps and $10^4$ thermalization steps were considered. To calculate the total average magnetization *M* at a specific temperature point, we used the next equation:

$$M = 2\mu_{\mathrm{Co}} m_{\mathrm{Co}} + \mu_{\mathrm{Cr}} m_{\mathrm{Cr}} , \qquad (2)$$

where $\mu_{\mathrm{Co}}$, and $\mu_{\mathrm{Cr}}$ are the magnetic moments of Co and Cr atoms, respectively.

## 2. Calculation results

Firstly, we determined the magnetic ground state of $Co_2CrIn$ Heusler alloy by calculating the total energies per formula unit as functions of the lattice parameter (see Fig. 2, *a*). Fig. 2, *a* shows that austenite structure with FM spin configuration is more energetically stable than FIM and AFM configurations. The energy minimum for FM austenite corresponds to equilibrium lattice parameter $a$ = 5,976 Å, the total magnetic moment is equal to 3,04 $\mu_B$/f.u. For FIM austenite both total magnetic moment 1,29 $\mu_B$/f.u. and equilibrium lattice parameter $a$ = 6,003 Å are close to the experimental data, 1,18 $\mu_B$/f.u. and 6,059 Å [5].

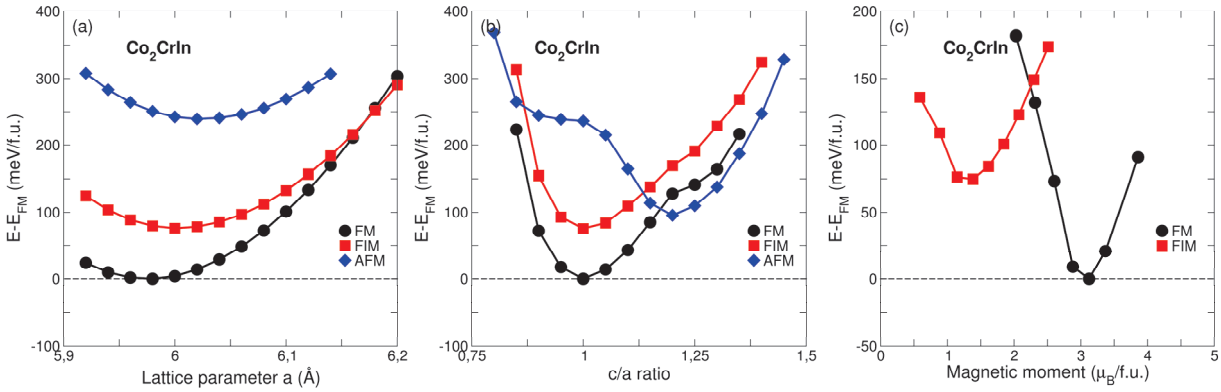


**Fig. 2. Dependence of total energy per formula unit on (a) lattice parameter, (b) tetragonality degree *c*/*a* and (c) fixed total magnetic moment of $Co_2CrIn$ alloy with FM, AFM, and FIM configurations. The energy difference was calculated with respect to the stable configuration (FM)**

To find a probability of martensitic transformation in this alloy, we calculated the dependency of the total energy, relative to the cubic phase, on tetragonality *c*/*a* (see Fig. 2, *b*). Fig. 2, *b* clearly demonstrates the absence of martensitic transformation in the stoichiometric $Co_2CrIn$ alloy. Therefore, we further present results only for the austenitic cubic state.

We also calculated the total energy of $Co_2CrIn$ as a function of a fixed magnetic moment for FM and FIM configurations (see Fig. 2, *c*). Fig. 2, *c* illustrates that FM configuration with the magnetic moment of ≈3 $\mu_B$/f.u. is more stable than FIM configuration (1,3 $\mu_B$/f.u.), which is close to experimental results [5].

The predicted lattice constants and magnetic moments for different magnetic states of $Co_2CrIn$ alloy, as well as available experimental data, are summarized in Table 1.

**Table 1**

**Optimized lattice constant $a_0$ (in Å), and total magnetic moment $\mu$ (in $\mu_B$/f.u.), for $Co_2CrIn$ alloy in comparison with experimental ($a_0^{exp}$, $\mu^{exp}$) and other theoretical ($a_0^{calc}$, $\mu^{calc}$) data**

| $a_0$ | $a_0^{exp}$ | $a_0^{calc}$ | $\mu$ | $\mu^{exp}$ | $\mu^{calc}$ |
|---|---|---|---|---|---|
| 5,976 (FM) | 6,0596 [5] | 6,00 [6] | 3,04 (FM) | 1,18 [5] | 3,16 [6] |
| 6,024 (AFM) | | | 0,50 (AFM) | | |
| 6,003 (FIM) | | | 1,29 (FIM) | | |

DOS calculations were performed for the cell with the optimized lattice constant, consisting of four atoms, by using SPR-KKR-CPA approach. Fig. 3 depicts total and partial DOS curves, calculated for $Co_2CrIn$ alloy with different magnetic reference states.

The most contributions to the majority and minority bands are caused by Co and Cr 3*d* states. In the case of FM configuration, the spin up band shows the metallic behaviour, while the spin down band demonstrates the semiconducting behaviour due to the appearance of an energy gap around the Fermi level. The resulting spin polarization is 76 %. As we mentioned above, the presence of both occupied majority spin-channel and unoccupied minority spin-channel at $E_F$ is the feature of the half-metallic behaviour. On the one hand, from element resolved DOS curves for FM configuration we can observe that the gap is larger for 3*d* states of Cr than of Co. On the other hand, the metallic behaviour (see the spin up band at $E_F$, Fig 3, *a*) is attributed to the hybridization between Cr and Co 3*d* states. In the cases of FIM and AFM configurations, the half-metallic behaviour changed to the metallic behaviour (energy gap around the Fermi level for the spin down band disappeared).

Since Co-based Heusler alloys are strongly correlated systems where the electron-electron correla-

tion can play a critical role, we studied the influence of Coulomb interaction on DOS curves, using GGA+*U* approach. We set the values of *U* and *J* for both Co and Cr atoms to 3 and 0,8 eV, respectively. Fig. 4 shows total DOS curves of $Co_2CrIn$ alloy near the Fermi level, calculated in GGA and GGA+*U* approximations.

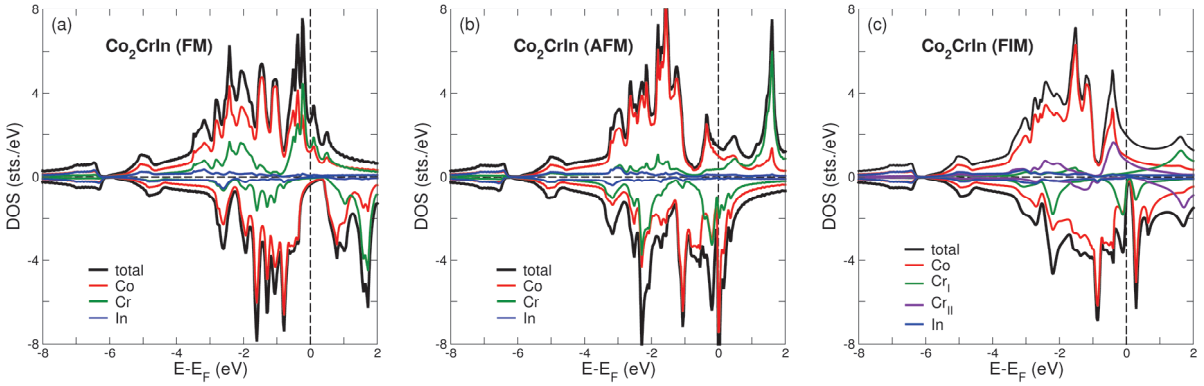


**Fig. 3. Total and partial DOS of $Co_2CrIn$ alloy for spin up and spin down bands: (a) FM, (b) AFM, and (c) FIM spin configurations**

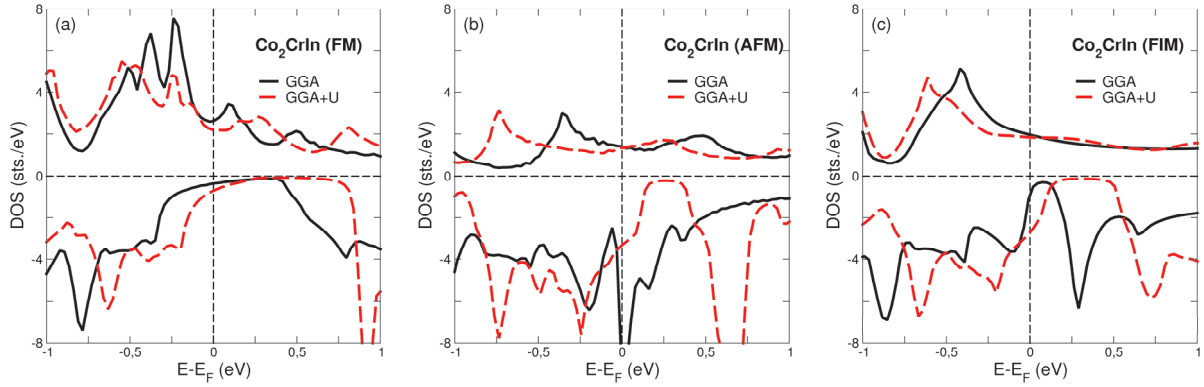


**Fig. 4. Total DOS curves for spin up and spin down bands of $Co_2CrIn$ alloy near the Fermi level in (a) FM, (b) AFM, and (c) FIM spin configurations. Solid (dashed) lines denote results for GGA (GGA+*U*) approach**

To estimate the spin polarization (*P*) from DOS curves, we used the next equation:

$$P = \frac{N\uparrow(E_F) - N\downarrow(E_F)}{N\uparrow(E_F) + N\downarrow(E_F)} \times 100\%. \quad (3)$$

The calculated spin polarizations *P* for different spin configuration of $Co_2CrIn$ alloy are listed in Table 2.

**Table 2**

**Spin polarization (*P*) of $Co_2CrIn$ alloy with FM, FIM, and AFM spin configurations, calculated in GGA and GGA+*U* approximations**

| Magnetic state | FM | AFM | FIM |
|---|---|---|---|
| GGA | 76,3 | – | 36,6 |
| GGA+*U* | 51,4 | 41,7 | 18,8 |

Fig. 4 shows that the addition of *U* term in DFT calculations practically did not change the majority bands around the Fermi level, while in the case of minority channel we can observe that Coulomb interaction results in the gap broadening. At the same time, the spin polarization generally decreased.

Further, we present the results of KKR-CPA calculations of exchange coupling parameters for $Co_2CrIn$ alloy with different magnetic configurations. Fig. 5 presents the dependence of magnetic exchange parameters for cubic $Co_2CrIn$ structure on the distance between atoms.

Fig. 5, *a* shows that in FM case Co-Cr pair demonstrates the largest exchange interaction between nearest neighbour atoms, while the interactions between Co-Co are slightly lower, and Cr-Cr atom pair interacts antiferromagnetically with a weak contribution to the total exchange energy. Overall, large FM Co-Cr and Co-Co interactions are responsible for the FM order and high Curie temperatures of austenite. In the case of FIM and AFM spin configurations, the trends of exchange integrals (see Fig. 5, *b*, *c*) are quite different, because in both cases nearest Co–Cr pairs have strong AFM interactions. As a result,

FIM and AFM $Co_2CrIn$ alloys demonstrate the competition between FM and AFM interactions, which vanishes with the increase of $d/a$ distance.

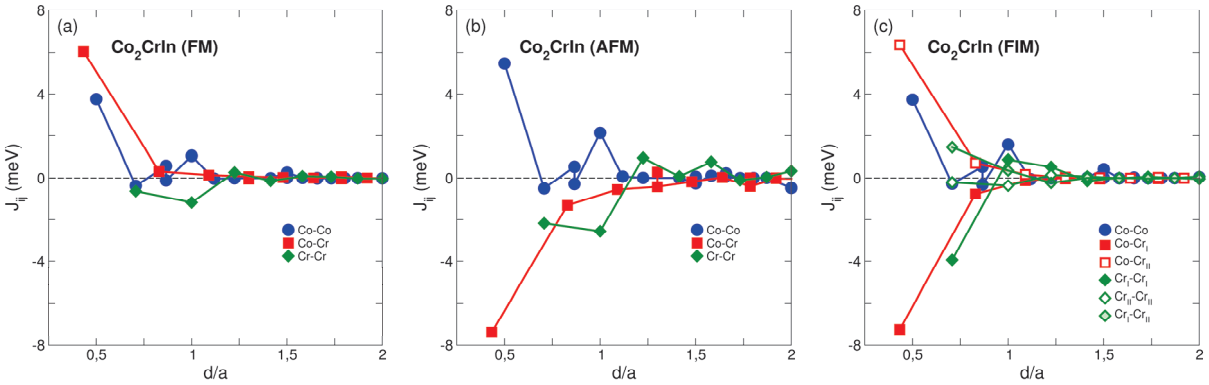


**Fig. 5. Dependence of exchange coupling parameters of $Co_2CrIn$ cubic structure with (a) FM, (b) AFM, and (c) FIM spin configuration on the distance ($d/a$) between atoms $i$ and $j$. We used the optimized lattice parameter for calculations**

To obtain the temperature dependencies of magnetization and specific heat curves for $Co_2CrIn$ alloy, we carried out MC simulations of classical three-dimensional Heisenberg model in the absence of anisotropy and magnetic fields [14]. In view of the fact that in all cases the similar ferromagnetic-paramagnetic phase transition behavior was observed we skip a discussion of this thermomagnetization curves in more detail here. Table 3 presents the results of MC calculations. For AFM spin configuration, the calculated temperature should be interpreted as Neel temperature. For comparison we also put temperatures, which obtained with the help of Mean-field approximation (MFA) for multicomponent system during SPR-KKR calculations according to P.W. Anderson [15]. It should be noted that the Curie temperature obtained within the MFA are higher than the Curie temperature obtained from the MC simulation, as shown in [16].

**Table 3**

**Calculated temperature of magnetic phase transition $T_C$ (in K) for $Co_2CrIn$ alloy with different magnetic configurations**

| Magnetic state | FM | AFM* | FIM |
|---|---|---|---|
| $T_C$(MC) | 335 | 600 | 174 |
| $T_C$(MFA) | 453 | 934 | 435 |

*In the case of AFM reference state, the calculated temperature should be treated as Neel temperature ($T_N$).

## Conclusion

In conclusion, the structural and magnetic properties of $Co_2CrIn$ Heusler compound have been studied by using the first-principles methods and Monte Carlo simulations. The first-principles calculations were carried out with the help of VASP and SPR-KKR simulations packages. Crystal structure optimization and fixed magnetic moment calculations have shown that the optimized ground state of Heusler $Co_2CrIn$ alloy with $L2_1$ structure is ferromagnetic. However, in the case of the ferrimagnetic state, where Cr atoms are ordered pairwise antiferromagnetically, calculated properties are close to experimental data. Energy calculations of tetragonal-type distortion of the cubic $L2_1$ structure for $Co_2CrIn$ have been demonstrated that the martensitic phase cannot be realized in the stoichiometric alloy. $Co_2CrIn$ alloy exhibits the pseudo-half-metallic behaviour only in the austenitic phase with the ferromagnetic order. Addition of Coulomb interaction decreases spin polarization. By using the calculated exchange coupling parameters in the Heisenberg Hamiltonian, we simulated the temperature dependences of magnetization. In general, we would like to emphasize that to the complete understanding of whole complex picture of the discussed problem, additional calculations for larger supercells and more different configurations of antisite disorder are needed.

## Acknowledgments

*This work was supported by Russian Science Foundation grant No. 17-72-20022 (Section 3) and Act 211 Government of the Russian Federation (contract No.02.A03.21.0011); VS acknowledges Ministry of Education and Science of the Russian Federation in the framework of increase Competitiveness Program of NUST "MISIS", implemented by a governmental decree dated 16th of March 2013, No 211.*

**References**

1. Comtesse D., Geisler B., Entel P., Kratzer P., Szunyogh L. First-principles study of spin-dependent thermoelectric properties of half-metallic Heusler thin films between platinum leads. *Phys. Rev. B*, 2014, Vol. 89, Issue 9, p. 094410. DOI: 10.1103/PhysRevB.89.094410

2. Felser C. (ed.), Fecher G.H. (ed.) *Spintronics: from Materials to Devices*. New York, Springer, 2013, 369 p. DOI: 10.1007/978-90-481-3832-6

3. Zagrebin M.A., Sokolovskiy V.V., Buchelnikov V.D. Electronic and magnetic properties of the $Co_2$-based Heusler compounds under pressure: first-principles and Monte Carlo studies. *Journal of Physics D: Applied Physics*, 2016, Vol. 49, no. 35, p. 355004. DOI: 10.1088/0022-3727/49/35/355004

4. Zagrebin M.A., Sokolovskiy V.V., Buchelnikov V.D., Pavlukhina O.O. Effect of structural disorder on the ground state properties of $Co_2CrAl$ Heusler alloy. *Physica B*, 2017, Vol. 519, pp. 82–89. DOI: 10.1016/j.physb.2017.05.039

5. Wurmehl S., Fecher G.H., Felser C. $Co_2CrIn$: A Further Magnetic Heusler Compound. *J. of Chemical Sciences*, 2006, Vol. 61, Issue 6, pp. 749–752. DOI: 10.1515/znb-2006-0615

6. Aly S.H., Shabara R.M. First principles calculation of elastic and magnetic properties of Cr-based full-Heusler alloys. *J. of Magnetism and Magnetic Materials*, 2014, Vol. 360, pp. 143–147. DOI: 10.1016/j.jmmm.2014.02.030

7. Kresse G., Joubert D. From ultrasoft pseudopotentials to the projector augmented-wave method *Phys. Rev. B*, 1999, Vol. 59, Issue 3, p. 1758. DOI: 10.1103/PhysRevB.59.1758

8. Kresse G., Furthműller J. Efficient iterative schemes for *ab initio* total-energy calculations using a plane-wave basis set. *Phys. Rev. B*, 1996, Vol. 54, Issue 16, pp. 11169–11186. DOI: 10.1103/PhysRevB.54.11169

9. Ebert H., Koedderitzsch D., Minar J. Calculating condensed matter properties using the KKR-Green's function method – recent developments and applications. *Reports on Progress in Physics*, 2011, Vol. 74, no. 9, p. 096501. DOI: 10.1088/0034-4885/74/9/096501

10. Perdew J.P., Burke K., Ernzerhof M. Generalized gradient approximation made simple. *Phys. Rev. Lett.*, 1996, Vol. 77, Issue 18, pp. 3865–3868. DOI: 10.1103/PhysRevLett.77.3865

11. Monkhorst H.J., Pack J.D. Special points for Brillonin-zone integrations. *Phys. Rev. B*, 1976, Vol. 13, Issue 12, pp. 5188–5192. DOI: 10.1103/PhysRevB.13.5188

12. Broyden C.G. A class of methods for solving nonlinear simultaneous equations. *Math. Comp*., 1965, Vol. 19, pp. 577–593. DOI: 10.1090/S0025-5718-1965-0198670-6

13. Press W.H., Teukolsky S.A., Vetterling W.T., Flannery B.P. *Numerical Recipes in Fortran*. Cambridge, Cambridge University Press, 1992, 963 p.

14. Landau D.P., Binder K. *A Guide to Monte Carlo Simulations in Statistical Physics*. Cambridge, Cambridge University Press, 2009, 488 p. DOI: 10.1017/CBO9780511994944

15. Anderson P.W. Theory of Magnetic Exchange Interactions: Exchange in Insulators and Semiconductors. *Solid State Physics*, 1963, Vol. 14, pp. 99–214. DOI: 10.1016/S0081-1947(08)60260-X

16. Zagrebin M.A., Derevyanko S.A., Sokolovskiy V.V., Buchelnikov V.D. Complex investigations of phase diagram of Ni-Pt-Mn-Ga Heusler alloys. *Letters on Materials*, 2018, Vol. 8, no. 1, pp. 21–26. DOI: 10.22226/2410-3535-2018-1-21-26

***Received January 9, 2019***

*Bulletin of the South Ural State University Series "Mathematics. Mechanics. Physics" 2019, vol. 11, no. 1, pp. 59–66*

**УДК 538.955** **DOI: 10.14529/mmph190108**

# ПЕРВОПРИНЦИПНЫЕ ИССЛЕДОВАНИЯ ОСНОВНЫХ СОСТОЯНИЙ СПЛАВОВ ГЕЙСЛЕРА $Co_2CrIn$

***М.А. Загребин[1,2,3], В.В. Соколовский[1,3], В.Д. Бучельников[1,3]***

*[1]Челябинский государственный университет, г. Челябинск, Российская Федерация*

*[2]Южно-Уральский государственный университет, г. Челябинск, Российская Федерация*

*[3]Национальный исследовательский технологический университет «МИСиС», г. Москва, Российская Федерация*

*E-mail: miczag@mail.ru*

Для выяснения причины различий между имеющимися теоретическими и экспериментальными значениями полного магнитного момента сплава Гейслера $Co_2CrIn$ в данной работе было изучено влияние различных основных магнитных состояний на магнитные и электронные свойства сплавов с помощью *ab initio* и Монте-Карло методов. Показано, что вычисленное основное состояние в фазе $L2_1$ является ферромагнитным. Однако равновесные значения как параметра решетки, так и магнитного момента, рассчитанные для ферримагнитного состояния, где атомы Cr упорядочены антиферромагнитно, находятся в хорошем согласии с имеющимися экспериментальными данными. Показано, что полуметаллическое поведение реализуется только в случае ферромагнитного упорядочения. Используя рассчитанные параметры обменного взаимодействия в гамильтониане Гейзенберга, были смоделированы температурные зависимости намагниченности.

*Ключевые слова: сплавы Гейслера; основные состояния; плотности состояний; обменные параметры.*

**Литература**

1. First-principles study of spin-dependent thermoelectric properties of half-metallic Heusler thin films between platinum leads / D. Comtesse, B. Geisler, P. Entel, P. Kratzer, L. Szunyogh // Phys. Rev. B. – 2014. – Vol. 89, Issue 9. – P. 094410.

2. Spintronics: from Materials to Devices / под ред. C. Felser, G.H. Fecher. – New York, USA: Springer, 2013. – 369 p.

3. Zagrebin, M.A. Electronic and magnetic properties of the $Co_2$-based Heusler compounds under pressure: first-principles and Monte Carlo studies / M.A. Zagrebin, V.V. Sokolovskiy, V.D. Buchelnikov // Journal of Physics D: Applied Physics. – 2016. – Vol. 49, no. 35. – P. 355004.

4. Effect of structural disorder on the ground state properties of $Co_2CrAl$ Heusler alloy / M.A. Zagrebin, V.V. Sokolovskiy, V.D. Buchelnikov, O.O. Pavlukhina // Physica B. – 2017. – Vol. 519. – P. 82–89.

5. Wurmehl, S. $Co_2CrIn$: A Further Magnetic Heusler Compound / S. Wurmehl, G.H. Fecher, C. Felser // J. of Chemical Sciences. – 2006. – Vol. 61, Issue 6. – P. 749–752.

6. Aly, S.H. First principles calculation of elastic and magnetic properties of Cr-based full-Heusler alloys / S.H. Aly, R.M. Shabara // J. of Magnetism and Magnetic Materials. – 2014. – Vol. 360. – P. 143–147.

7. Kresse, G. From ultrasoft pseudopotentials to the projector augmented-wave method / G. Kresse, D. Joubert // Phys. Rev. B. – 1999. – Vol. 59, Issue 3. – P. 1758.

8. Kresse, G. Efficient iterative schemes for *ab-initio* total-energy calculations using a plane-wave basis set / G. Kresse, J. Furthműller // Phys. Rev. B. – 1996. – Vol. 54, Issue 16. – P. 11169–11186.

9. Ebert, H. Calculating condensed matter properties using the KKR-Green's function method – recent developments and applications / H. Ebert, D. Koedderitzsch, J. Minar // Reports on Progress in Physics. – 2011. – Vol. 74, no. 9. – P. 096501.

10. Perdew, J.P. Generalized gradient approximation made simple / J.P. Perdew, K. Burke, M. Ernzerhof // Phys. Review Lett. – 1996. – Vol. 77, Issue 18. – P. 3865–3868.

11. Monkhorst, H.J. Special points for Brillonin-zone integrations / H.J. Monkhorst, J.D. Pack // Phys. Rev. B. – 1976. – Vol. 13, Issue 12. – P. 5188–5192.

12. Broyden, C.G. A class of methods for solving nonlinear simultaneous equations / C.G. Broyden // Math. Comp. – 1965. – Vol. 19. – P. 577–593.

13. Numerical Recipes in Fortran / W.H. Press, S.A. Teukolsky, W.T. Vetterling, B.P. Flannery. – Cambridge, United Kingdom: Cambridge University Press, 1992. – 963 p.

14. Landau, D.P. A Guide to Monte Carlo Simulations in Statistical Physics / D.P. Landau, K. Binder. – Cambridge, United Kingdom: Cambridge University Press, 2009. – 488 p.

15. Anderson, P.W. Theory of Magnetic Exchange Interactions: Exchange in Insulators and Semiconductors / P.W. Anderson // Solid State Physics. – 1963. – Vol. 14. – P. 99–214.

16. Complex investigations of phase diagram of Ni-Pt-Mn-Ga Heusler alloys / M.A. Zagrebin, S.A. Derevyanko, V.V. Sokolovskiy, V.D. Buchelnikov // Letters on Materials. – 2018. – Vol. 8, no. 1. – P. 21–26.

***Поступила в редакцию 9 января 2019 г.***